Protein Science (1999), *8*:985–990. Cambridge University Press. Printed in the USA.
Copyright © 1999 The Protein Society

Evidence for a copper-coordinated histidine–tyrosine cross-link in the active site of cytochrome oxidase

GERHARD BUSE,[1] TEWFIK SOULIMANE,[1] MANFRED DEWOR,[1] HELMUT E. MEYER,[2] AND MARTIN BLÜGGEL[2]

[1]Institut für Biochemie, Rheinisch-Westfälische Technische Hochschule Aachen, Pauwelsstrasse 30, 52074 Aachen, Germany
[2]Institut für Immunologie, Ruhr, Universität Bochum, 44780 Bochum, Germany

(RECEIVED October 26, 1998; ACCEPTED January 19, 1999)

Abstract

Following hints from X-ray data (Ostermeier C et al., 1997, *Proc Natl Acad Sci USA 94*:10547–10553; Yoshikawa S et al., 1998, *Science 280*:1723–1729), chemical evidence is presented from four distantly related cytochrome-*c* oxidases for the existence of a copper$_B$-coordinated His240–Tyr244) cross-link at the O_2-activating Heme Fea_3–Cu$_B$ center in the catalytic subunit I of the enzyme. The early evolutionary invention of this unusual structure may have prevented demaging $^{\bullet}$OH-radical release at e^--transfer to dioxygen and thus have enabled O_2 respiration.

Keywords: cell respiration; cytochrome-*c* oxidase; histidine–tyrosine cross-link; O_2 activation; oxygen radicals

Cytochrome *c* oxidase [EC.1.9.3.1] is the main enzyme in the animated world for the respiration of dioxygen. The enzyme is located in the inner membrane of mitochondria in eucaryotes and in the plasma membrane of aerobic bacteria. It catalyzes the reduction of dioxygen according to the equation:

$$4\ \text{Cyt-}c^{Fe2+} + (4 + n)H_i^+ + O_2 = 4\ \text{Cyt-}c^{Fe3+} + nH_o^+ + 2H_2O \quad (1)$$

where H_i^+ and H_o^- represent protons at the inner and outer sides of the membrane (Babcock & Wikström, 1992; Rich, 1995). The exergonic O_2-reaction thus enables a vectorial consumption and outward pumping of H^+, thereby contributing to the electrochemical potential over the membrane that is mainly consumed for ATP synthesis.

Subunit I of the oligomeric enzyme (complex IV of the respiratory chain) contains an electron transferring heme and the catalytic heme a_3–Cu$_B$ center invariably coordinated to a set of six histidine residues of the protein (Ferguson-Miller & Babcock, 1996). Part of the reaction at this center is the activation of dioxygen according to the equation:

$$4e^- + 4H^+ + O_2 = 2H_2O \quad (2)$$

with the inherent difficulty of successively transferring electrons and protons to dioxygen without release of the dangerous superoxide anion radical $^{\bullet}O_2^-$, the peroxide O_2^{2-} and especially the extremely poisonous hydroxyl radical $^{\bullet}$OH from the peroxide split.

Structural and functional knowledge about the mitochondrial and bacterial oxidases has accumulated during the last decades, and was recently confirmed by two high resolution X-ray structures obtained from a mitochondrial (Tsukihara et al., 1995) and a bacterial (Iwata et al., 1995) enzyme. The necessary primary structures for these X-ray models had been obtained either from the proteins, mostly by our group (Buse et al., 1987) or deduced from the genes (Anderson et al., 1982; Van der Oost et al., 1991). Especially for the large 57- to 66-kDa subunits I there exists no complete protein sequence (Hensel & Buse, 1990).

Although both originally published X-ray structures do not show unusual aspects concerning the active center, S. Yoshikawa, at the 1997 Gordon Research Conference, presented a 2.3 Å refinement of the bovine enzyme with the copper complexing His240 and invariant Tyr244 side chains approached to a distance of a covalent bridge between the imidazol Nϵ2 and the Cϵ2 of the phenol ring (Yoshikawa et al., 1998). Also, H. Michel and coworkers, on refining the structure of the *Paracoccus* enzyme, found the observed electron density to be in better agreement with a covalent cross-link (Ostermeier et al., 1997). Because, however, from the X-ray data a decision of this question was not possible, both authors demanded a protein chemical analysis of this unusual structure.

We have used the 13-subunit bovine and the 2-subunit *Paracoccus denitrificans* aa_3–cytochrome-*c* oxidases and the caa_3– and ba_3–cytochrome-*c* oxidases from *Thermus thermophilus*, two two-subunit enzymes, where cytochrome-*c*/subunit II and subunit I/III are expressed as fused proteins and heme *b* substitutes heme *a*, respectively (Buse et al., 1989; Keightley et al., 1995) for this analysis.

Reprint requests to: Gerhard Buse, Institut für Biochemie, RWTH Aachen, Pauwelsstrasse 30, 52074 Aachen, Germany; e-mail: Gerhard Buse@post.rwth-aachen.de.

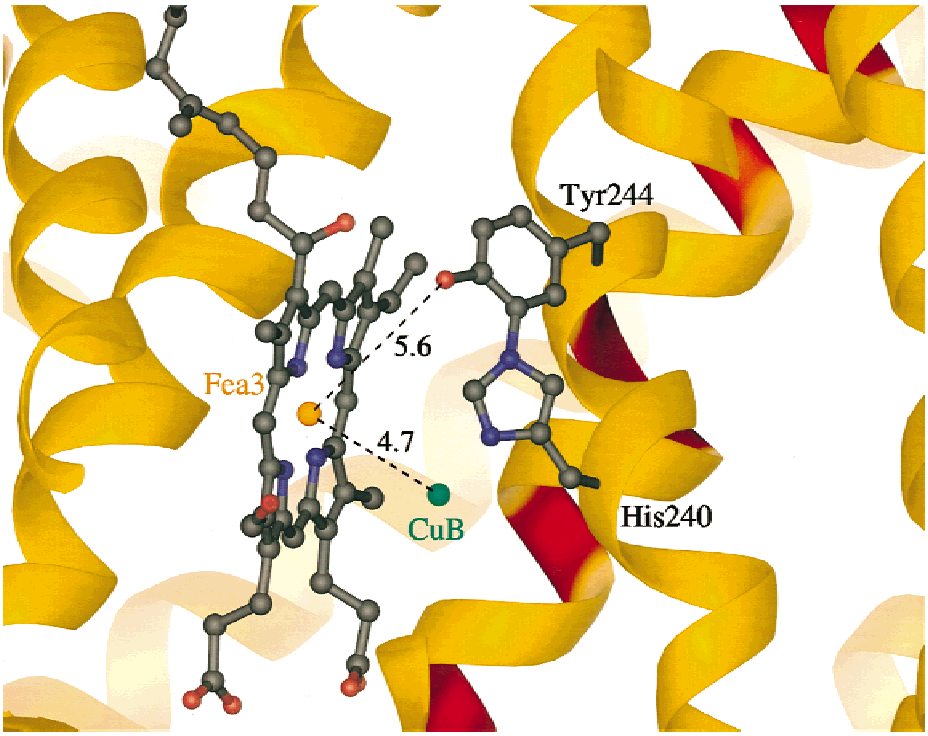

Fig. 1. The covalent histidine–tyrosine bond brings the tyrosine–OH in proper position (Fe ↔ O distance 5.6 Å) for reacting with the Fea_3–peroxy intermediate (**P**, not visible) identified in the catalytic cycle of the oxidase (Babcock & Wikström, 1992). Modeling has been performed on the basis of the published X-ray structure (Tsukihara et al., 1996) with the program "Ribbons" (Carson, 1991).

Results

To study the situation we have modeled the active site under the assumption of an existing covalent bridge on the basis of the published 2.8 Å coordinates (Tsukihara et al., 1996) without changing the positions of the heme a_3–iron, the $copper_B$, and the membrane helix VI. The modeling shows that the $copper_B$ must be Nδ-coordinated at His240; the imidazol Nϵ then fits to the Cϵ of the Tyr244 phenol only. Another requirement for the covalent bridge is Pro241, which introduces a slight distortion of the membrane helix enabling the His240 and Tyr244 side chains to contact (Fig. 1). The model displays a distance of 5.6 Å between the oxygen of the tyrosine–OH and the heme a_3 iron, suitable for interacting with a peroxy intermediate at the heme a_3–iron. This intermediate has been identified in the catalytic cycle of the enzyme (Wikström, 1989; Babcock & Wikström, 1992); however, it cannot be identified from the X-ray data at the present resolution.

To reach at the sequence positions His240 and Tyr244 (bovine numbering) in the middle of the 514 to 594 residues polypeptides, we used a limited acid hydrolysis of the sensitive Asp227–Pro228 bond, which is invariably positioned 13 residues N-terminal of His240 in the four polypeptides (see also Fig. 5 below). In the case of the bovine, *Paracoccus* and *Thermus* caa_3–enzymes, the limited proteolytic cleavage resulted mainly in large fragments of the polypeptides having N-terminal proline because the subunits are N-terminally blocked. The fragments could easily be separated and sequenced. In the *Thermus* ba_3 subunit I (Keightley et al., 1995), a second site at residues Asp269–Pro270 of the chain is cleaved as well, resulting in a 42-residue peptide that covers the sequence in question, and could be purified in nmol amounts by reversed phase HPLC (Fig. 2).

Sequencing of the C-terminal halve fragments of the bovine, *Paracoccus*, and *Thermus* caa_3 subunit I starting from Pro228 showed in all cases clearly the expected amino acid sequences (see Fig. 5) with gaps, i.e., no new phenylthiohydantoin (PTH)–amino acids emerging at cycles 13 and 17 of the sequences. Neither histidine nor tyrosine or any other amino acid could be identified in the corresponding positions; all other residues of this segment were clearly identified as deduced from the gene sequences.

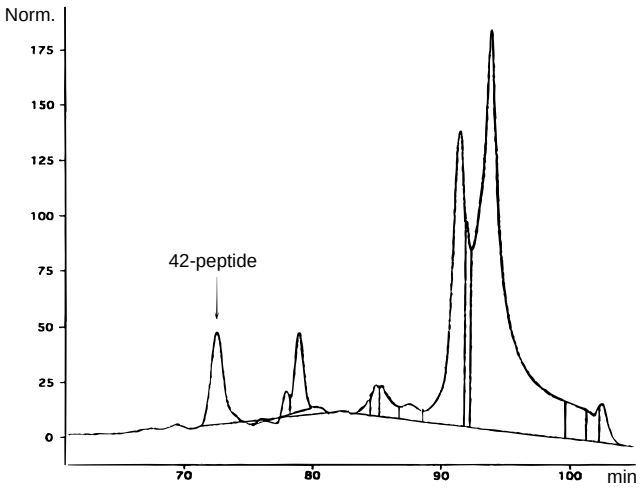

Fig. 2. Purification by rpHPLC of the 42-residue fragment obtained from limited proteolytic cleavage at Asp–Pro peptide bonds of the *Thermus*–ba_3 oxidase subunit I.

In the case of the 42-residue *Thermus* ba_3 subunit I fragments from the reduced and the oxidized enzyme, we performed sequence runs with up to 4 nmol of the peptide. Although the instrument is normally used with low pmol amounts, we obtained the deduced sequences, but no PTH–histidine or PTH–tyrosine at cycles 13 and 17 emerged, respectively. The protein sequence confirmed isoleucine in the bovine homologue position Glu242, a functionally important amino acid exchange as compared to the proton pumping bovine and *Paracoccus* oxidases (Fig. 3).

The purified 42-residue *Thermus* ba_3–peptide was used for a mass determination with an electrospray mass spectrometer that can safely discriminate two mass units in a molecular mass of about 5,000 Da (Fig. 4). The average mass of the peptide is 4,816.76 Da, calculated from the deduced sequence. The molecular weight of the peptide was determined from the masses observed for the peptide in the charge states 4, 5, 6, and its formyl derivatives. All in all, 18 masses were averaged to the mass of 4,814.8 ± 0.4 Da as expected if a covalent bond has removed 2H. A peptide fragmentation spectrum was recorded by the ion selection of the $[M+MH]^{4+}$-ion with the m/z value 1,204.8. The fragmentation pattern verifies the sequence of the peptide and due to the double charged *b*-ion series the mass shift of 2 Da was localized in the 17 N-terminal amino acids (228–244) containing His240 and Tyr244 of this 42 amino acid's long peptide. The mass spectrum shows no evidence for the presence of any other peptide. In agreement with the data from protein sequencing, the existence of a 4,816.8 Da species, i.e., a peptide without cross-linked His240 and Tyr244 residues, is thus excluded.

We understand these results as: (1) Evidence for the existence of a covalent His240–Tyr244 cross-link in the oxygen-reducing center of this enzyme family. (2) Evidence against a formation and opening of the bond in the catalytic cycle, because both the oxidized and the reduced enzyme preparation contain the cross-link. (3) An indication that this structure is important for the catalytic oxygen activating mechanism itself, i.e., reaction Equation 2, because the covalently fixed tyrosine side chain may be unsuitable for gating H^+-transferring conformational energy of a proton pump. (4) As evidence against an artefact resulting from the high-energy X-ray treatment of the crystals in the presence of O_2, copper, iron, and the susceptible histidine and tyrosine side chains, because active preparations also contain nothing other than the cross-linked species.

The covalent N–C bond, as shown in Figure 1, should be more stable against acid hydrolysis than a peptide bond. Correspondingly, we have discovered a small unknown peak in the amino acid analyses of subunits I running behind the normal histidine in the cation exchange separation (not shown). This species copurifies with amino acid analyses of the 4,814 Da (42 residues) peptide and is absent in other amino acid analyses, for example, of subunits II or subunits III of the oxidases. We have seen a mass signal at 568 Da in the eluate of the 17. sequencing cycle of the 42-residue peptide that may correspond to bis-PTH-His-Tyr, and a mass signal at 334 Da in the amino acid hydrolysates of the peptide and subunit I that would correspond to the His/Tyr product. These signals are, however, not of similar significance as those of the 42-residue peptide itself, because there is a vast array of signals in the low M_r range of the mass spectra.

Discussion

To our knowledge, a covalent copper-coordinated His–Tyr cross-link has so far not been described in biochemistry. However, a few covalently modified tyrosine residues have been found especially in copper proteins, for instance, a Cys–Tyr linkage in the active site of galactose oxidase (Ito et al., 1994) and a 2,4,5-trihydroxyphenylalanine quinone in amine oxidase (Parsons et al., 1995). Nothing is known about the synthesis of the His–Tyr cross-link in cytochrome-*c* oxidase. We consider the possibility of a nonenzymatic formation by oxygen radical mechanisms in the presence of the electron-donating metals of the biosynthesized enzyme. The imidazol and phenol rings of histidine and tyrosine are among the most susceptible side chains for radical reactions of the protein amino acids (Davies et al., 1987). The enzyme thus may activate itself. Experiments are in progress to show whether in a synthetic peptide the cross-link can be formed under oxygen radical conditions in the presence of iron and copper ions.

The existence of the His–Tyr cross-link in the catalytic center of the enzyme must be meaningful. According to sequence align-

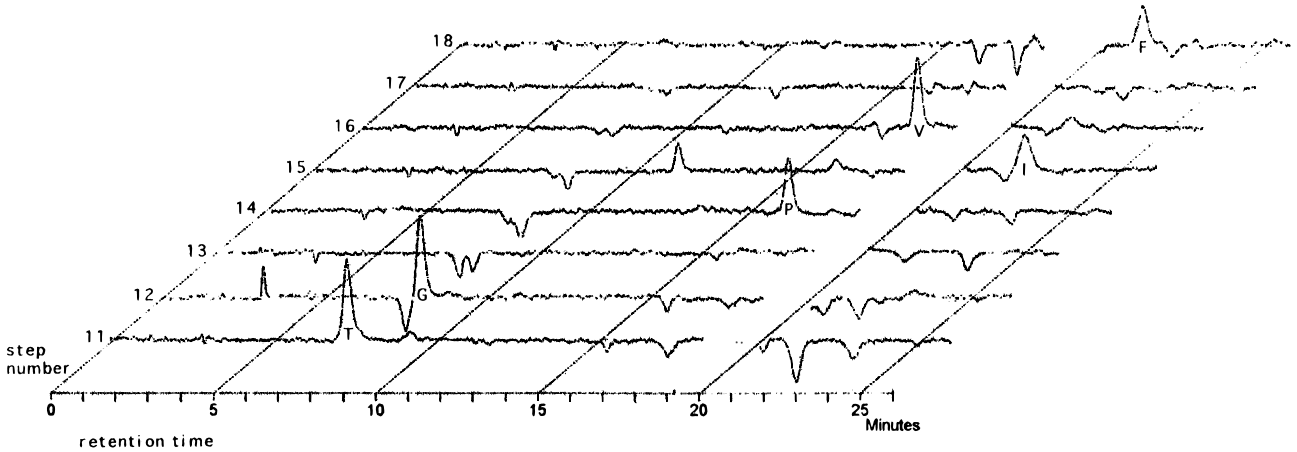

Fig. 3. Amino acid sequence at the covalent His–Tyr cross-link shows the gene-deduced sequences but no (PTH-) histidine and tyrosine at cycles 13 and 17, respectively, of the peptide. The chromatogram of the previous cycle has been subtracted from the actual using the Knauer "WinSeq" Program.

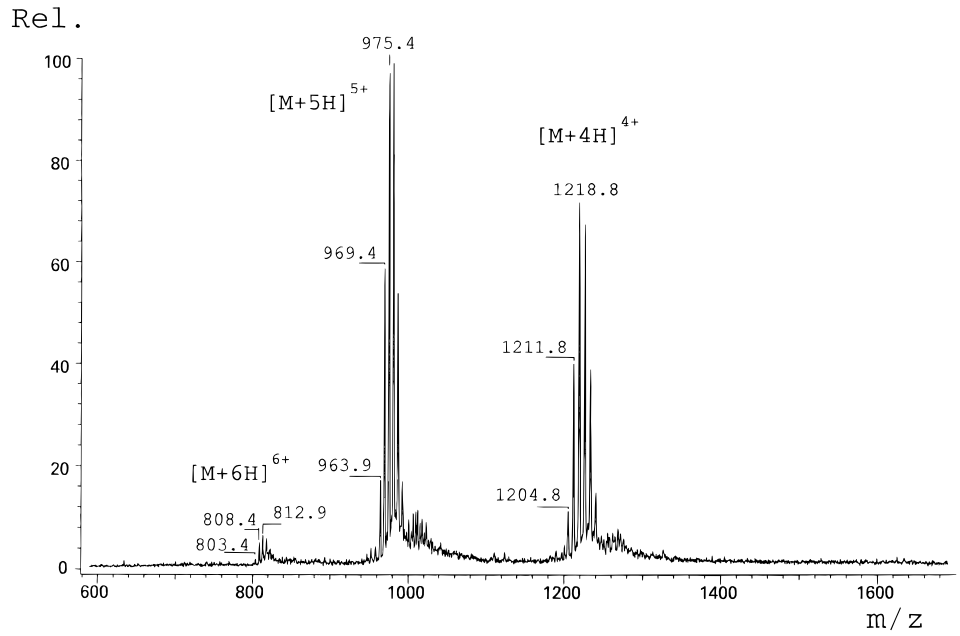

Fig. 4. Mass spectrum of the 42-residue fragment from subunit I of *Thermus th*. ba_3–oxidase. The molecular weight of 4,814.8 Da for the cross-linked His240–Tyr244 peptide can be calculated from the charge states 4, 5, and 6 as well as from the formyl derivatives (0–5).

ments, the -His-Pro-x-Val-Tyr- motif is present in all cytochrome *c* and quinol oxidases of eucaryotes (mitochondria), eubacteria, and archaea, respectively. It is, however, not found in the very distantly related so-called fixN terminal heme, copper oxidases, which are expressed during nitrogen fixation in root nodules (Preisig et al., 1993). The catalytic subunit of NO-reductase [EC.1.7.99.7] is homologous to subunit I of cytochrome oxidase, and contains the canonical histidine residues in place for coordination of two heme irons and a copper (Zumft, 1993). However, nonheme iron has been found instead of $copper_B$, and the Pro241 and Tyr244 homologous positions are occupied by other residues. Figure 5 shows the sequences around the membrane helix VI of subunit I of the four distantly related cytochrome-*c* oxidases in which the bridging structure has been found aligned to one fixN oxidase and one NO-reductase. Irrespective of probably different mechanisms of energy conservation (Musser & Chan, 1998; Kannt et al., 1998), all members of the respiratory oxidases including those phylogenetically reaching back to the thermophilic era (Stetter, 1996; Deckert et al., 1998) seem to contain this structure, which first may have enabled O_2 depoisoning reactions and later achieved its meaning for energy conserving respiration.

We suggest that the electron-donating properties of the connected conjugated ring system (Fig. 6) depend on the oxidation state of the imidazol Nδ-coordinated $copper_B$. The tyrosine–OH then may transfer a hydrogen atom to the terminal oxygen of the peroxy compound (**P**) (Wikström, 1989) in the catalytic cycle, induce its cleavage by formation of a OH^-–ion, preventing $^{\bullet}OH$ radical formation. The electron gap at the conjugated ring system can be filled from the $copper_B$, and a proton can be accepted to complete the phenol. The immediate advantage of this mechanism would be that a separate e^-, H^+ transfer does not occur at a released but at a bound oxygen atom, and thus cannot liberate $^{\bullet}OH$ radicals.

The existence of this structure in the active site of cytochrome oxidase gives a new basis for the interpretation and reinvestigation of spectroscopic and kinetic data that may help to understand the enzyme's catalytic mechanism (Proshlyakov et al., 1998).

```
          227          240 244                          270
           ↓            ┌──┐
Bh aa3    DPILYQHLFW FFGHPEVYIL ILPGFGMISH IVTYYSGKKE PFGY
           ↓
Pd aa3    DPVLYQHILW FFGHPEVYII ILPGFGIISH VISTFAKKPI  FGY
           ↓
Tt caa3   DPVLFQQFFW FYSHPTVYVM LLPYLGILAE VASTFARKPL  FGY
           ↓                                            ↓
Tt ba3    DPLVARTLFW WTGHPIVYFW LLPAYAIIYT ILPKQAGGKL VSDP

Bd fixN   GGIQDAMFQW WYGHNAVGFF LTAGFLAIMY YFIPKRAERP IYSY

Ps NO-red NLSRDKFYWW FVVHLWVEGV WELIMGAMLA FVLIKVTGVD REVI
          ++       *    *+ *+    ++
```

Fig. 5. Comparison of membrane helix VI amino acid sequences with His240 and Tyr244 cross-link of subunits I from four cytochrome *c* oxidases with one FixN oxidase and nitric oxide reductase. Bovine heart aa_3–oxidase (Bh aa_3) (AOO464); *P. denitrificans* aa_3–oxidase (Pd aa_3) (C35121); *T. thermophilus* caa_3–oxidase (Tt caa_3) (A46616); *T. thermophilus* ba_3–oxidase (Tt ba_3) (LO9121); *Bradyrhizobium japonicum fixN*-oxidase (Bd *fixN)* (A47468); *Pseudomonas stutzeri* NO-reductase (Ps NO-red) (S41117). ↓ Asp–Pro cleavage site. Accession numbers (Protein Identification Resource databank) in parentheses. *Conserved; +conserved in respiratory cytochrome *c* and quinol oxidases.

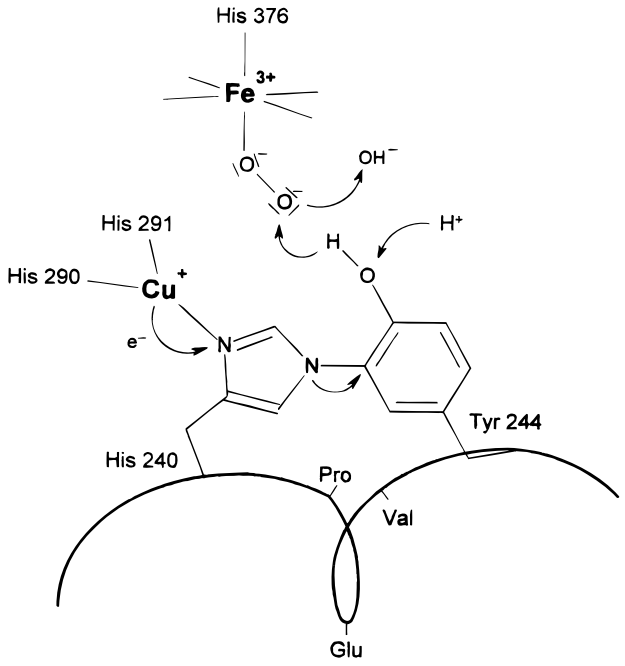

Fig. 6. Proposed reaction mechanism for the peroxy-split at the heme Fea_3–Cu_B center of cytochrome *c* oxidase. The H-atom at Tyr244 is transferred to the heme Fea_3-bound peroxy species to release an OH^--anion. The electron gap is filled from the Cu_B^{1+} and H^+ is added to restore the tyrosine–OH.

Materials and methods

Enzyme preparation

The bovine and *Paracoccus denitrificans* aa_3–cytochrome-*c* oxidases were isolated as described (Steffens et al., 1993; Soulimane & Buse, 1995). The ba_3- and caa_3-type cytochrome-*c* oxidases from *T. thermophilus* were prepared according to previously published procedures (Buse et al., 1989; Soulimane et al., 1995) as normal oxidized and as dithionite reduced enzymes.

Subunit separation

Subunit I of the bovine heart and *P. denitrificans* enzymes were isolated by BioGel-P100 chromatography in 3% sodiumdodecylsulfate as described previously by Buse et al. (1986). The subunits I of the *Thermus* oxidized and dithionite reduced ba_3 and caa_3 oxidases were purified on a reversed-phase Synchropak C_4 column (250 × 4.6 mm) using high-performance liquid chromatography (Hewlett Packard 1050 with multidiode array detection) in a gradient of: (1) 60% formic acid, 40% water and (2) 60% formic acid, 20% acetonitril, 15% *n*-propanol, and 5% water.

Aspartyl–prolyl cleavage and isolation of the peptides

The cleavage at the acid labile aspartic acid–proline peptide bonds was performed with nmol amounts of the polypeptides in 1 mL 75% formic acid for 15 h at 45 °C. The reaction mixture was then evaporated to dryness under reduced pressure, and the peptides dissolved in buffer A of the rpHPLC (20% formic acid, 20% acetonitril, 60% water) and separated on a Synchropac RP-4 column at 30°C, flow rate 0.70 mL/min in B (20% formic acid, 78% acetonitril, 2% water) with a gradient of 0, 40, and 100% B at 0, 60, and 90 min, respectively.

Amino acid analysis and sequencing

Quantitative amino acid analyses of the subunits and peptides were performed on a Biotronik amino acid analyzer LC 5001 equipped with a fluorescence detection of *o*-phtalaldehyde derivatives. The protein sample was hydrolyzed in 5.7 N HCl containing 0.2% thioglycolic acid for 90 min at 150 °C. Less reliable and non-determined amino acids, such as cysteine and tryptophan, were not considered in case of calculation of the protein concentration.

Automated N-terminal sequencing was carried out in a Knauer 910 gas/liquid-phase protein sequencer on polyvinylidenfluorid membranes with autoconversion and on-line HPLC identification of the phenylthiohydantoin amino acids.

Mass spectrometry

Electrospray mass spectrometry (ESI-MS) was performed on a triple-stage quadrupole mass spectrometer (Finnigan MAT TSQ 7000, Bremen) equipped with an in-house build nanospray source. The spectrum (Fig. 4) was averaged for 4 min. The collision-induced dissociation experiment was done by selecting the $[M+4H]^{4+}$-ion in the first mass analyzer (m/z 1,204.8) and passing the ion into a collision cell filled with argon (3 mTorr). The third quadrupole was scanned from m/z 40 to 2,500 Da at 10 s/scan. The spectrum was averaged for 15 min.

Modeling

Modeling of the structures of the O_2-activating center of cytochrome-*c* oxidase has been done on the basis of the published structural data of the bovine oxidase (Tsukihara et al., 1996) with the program "Ribbons" (Carson, 1991).

Supplementary material in Electronic Appendix

Contains data on mass calculation and MS fragmentation.

Acknowledgments

We thank Dr. J. Grötzinger (Aachen) for the modeling of Figure 1, Dr. S. Yoshikawa (Hyogo) for sending the 2.3 Å data prior to publication, and the Deutsche Forschungsgemeinschaft for supporting this work (Bu 463/3-2 and Me 765/3-4).

References

Anderson S, de Bruin M, Carlson A, Eperon I, Young IG. 1982. Complete sequence of bovine mitochondrial DNA. Conserved features of the mammalian mitochondrial genome. *J Mol Biol 156*:683–718.

Babcock GT, Wikström M. 1992. Oxygen activation and the conservation of energy in cell respiration. *Nature 356*:301–309.

Buse G, Hensel S, Fee JA. 1989. Evidence for cytochrome oxidase subunit I and a cytochrome *c* subunit II fused protein in the cytochrome c_1aa_3 of *Thermus thermophilus. Eur J Biochem 181*:261–268.

Buse G, Steffens GCM, Biewald R, Bruch B, Hensel S. 1987. Respiratory complex IV and cytochrome a,a_3. In: Papa S, Chance B, Ernster L, eds. *Cytochrome systems.* New York: Plenum Publishing Corp. pp 261–270.

Buse G, Steffens GJ, Steffens GCM, Meinecke L, Hensel S, Reumkens J. 1986. Sequence analysis of complex membrane proteins (cytochrome *c* oxidase).

In: Wittmann-Liebold B, ed. *Advanced methods in protein microsequence analysis*. Berlin: Springer Verlag. pp 340–351.
Carson M. 1991. Ribbons 2.0. *Appl Crystallogr 24*:946–950.
Davies KJA, Delsignore ME, Lin SW. 1987. Protein damage and degradation by oxygen radicals II. Modification of amino acids. *J Biol Chem 262*:9902–9907.
Deckert G, Warren PV, Gaasterland T, Young WG, Lenox AL, Gaham DE, Overbeek R, Snead MA, Keller M, Aujay M, Huber R, Feldman RA, Short JM, Olson GJ, Swanson RV. 1998. The complete genome of the hyperthermophilic bacterium *Aquifex aeolicus*. *Nature 392*:353–358.
Ferguson-Miller S, Babcock GT. 1996. Heme/copper terminal oxidases. *Chem Rev 96*:2889–2907.
Hensel S, Buse G. 1990. Studies on cytochrome-*c* oxidase, XIV. The amino-acid sequence of subunit I—Proteinchemical methods for the analysis of a large hydrophobic membrane protein. *Biol Chem Hoppe-Seyler 371*:411–422.
Ito N, Phillips SEV, Yadav KDS, Knowles YPF. 1994. Crystal structure of a free radical enzyme, galactose oxidase. *J Mol Biol 238*:794–814.
Iwata S, Ostermeier C, Ludwig B, Michel H. 1995. Structure at 2.8 Å resolution of cytochrome *c* oxidase from *Paracoccus denitrificans*. *Nature 376*:660–669.
Kannt A, Soulimane T, Buse G, Becker A, Bamberg E, Michel H. 1998. Electrical current generation and proton pumping catalysed by the ba_3-type cytochrome *c* oxidase from *Thermus thermophilus*. *FEBS Lett 434*:17–22.
Keightley JA, Zimmermann BH, Mather MW, Springer P, Pastuszyn A, Lawrence DM, Fee JA. 1995. Molecular genetic and protein chemical characterisation of the cytochrome ba_3 from *Thermus thermophilus* HB8. *J Biol Chem 270*:20345–20358.
Musser SM, Chan SI. 1998. Evolution of the cytochrome *c* oxidase proton pump. *Mol Evol 46*:508–520.
Ostermeier C, Harrenga A, Ermler U, Michel H. 1997. Structure at 2.7 Å resolution of the *Paracoccus denitrificans* two-subunit cytochrome *c* oxidase complexed with an antibody Fv fragment. *Proc Natl Acad Sci USA 94*:10547–10553.
Parsons MR, Convery MA, Wilmot CM, Yadav KDS, Blakeley V, Corner AS, Phillips SEV, McPherson MJ, Knowles PF. 1995. Crystal structure of a quinoenzyme: Copper amine oxidase of *Escherichia coli* at 2 Å resolution. *Structure 3*:1171–1184.
Preisig O, Anthamatten D, Hennecke H. 1993. Genes for a microaerobically induced oxidase complex in *Bradyrhizobium japonicum* are essential for a nitrogen-fixing endosymbiosis. *Proc Natl Acad Sci USA 90*:3309–3313.
Proshlyakov DA, Pressler MA, Babcock GT. 1998. Dioxygen activation and bond cleavage by mixed-valence cytochrome *c* oxidase. *Proc Natl Acad Sci USA 95*:8020–8025.
Rich PR. 1995. Towards an understanding of the chemistry of oxygen reduction and proton translocation in iron-copper respiratory oxidases. *Aust J Plant Physiol 22*:479–486.
Soulimane T, Buse G. 1995. Integral cytochrome-*c* oxidase: Preparation and progress towards a three-dimensional crystallisation. *Eur J Biochem 227*:588–595.
Soulimane T, Gohlke U, Huber R, Buse G. 1995. Three-dimensional crystals of cytochrome-*c* oxidase from *Thermus thermophilus* diffracting to 3.8 Å resolution. *FEBS Lett 368*:132–134.
Steffens GCM, Soulimane T, Wolff G, Buse G. 1993. Stoichiometry and redox behaviour of metals in cytochrome-*c* oxidase. *Eur J Biochem 213*:1149–1157.
Stetter KO. 1996. Hyperthermophiles in the history of life. *Ciba Found Symp 202*:1–10.
Tsukihara T, Aoyama H, Yamashita E, Tomizaki T, Yamaguchi H, Shinzawa-Itoh K, Nakashima R, Yaono R, Yoshikawa S. 1995. Structures of metal sites of oxidised cytochrome *c* oxidase at 2.8 Å. *Science 269*:1069–1074.
Tsukihara T, Aoyama H, Yamashita E, Tomizaki T, Yamaguchi H, Shinzawa-Itoh K, Nakashima R, Yaono R, Yoshikawa S. 1996. The whole structure of the 13-subunit oxidised cytochrome *c* oxidase at 2.8 Å. *Science 272*:1136–1144.
Van der Oost J, Haltia T, Raitio M, Saraste M. 1991. Genes coding for cytochrome *c* oxidase in *Paracoccus denitrificans*. In: Azzi A, ed. *Journal of bioenergetics and biomembranes 23*. New York: Plenum Press. pp 257–267.
Wikström M. 1989. Identification of the electron transfers in cytochrome oxidase that are coupled to proton-pumping. *Nature 338*:776–778.
Yoshikawa S, Shinzawa-Itoh K, Nakashima R, Yaono R, Yamashita E, Inoue N, Yao M, Fei MJ, Libeu CP, Mizushima T, Yamaguchi H, Tomizaki T, Tsukihara T. 1998. Redox-coupled crystal structural changes in bovine heart cytochrome *c* oxidase. *Science 280*:1723–1729.
Zumft WG. 1993. The biological role of nitric oxide in bacteria. *Arch Microbiol 160*:253–264.